BASIC RESEARCH www.jasn.org

Integration of Cistromic and Transcriptomic Analyses Identifies *Nphs2*, *Mafb*, and *Magi2* as Wilms' Tumor 1 Target Genes in Podocyte Differentiation and Maintenance

Lihua Dong,* Stefan Pietsch,* Zenglai Tan,* Birgit Perner,* Ralph Sierig,* Dagmar Kruspe,* Marco Groth,† Ralph Witzgall,‡ Hermann-Josef Gröne,§ Matthias Platzer,† and Christoph Englert*‖

Departments of *Molecular Genetics and †Genome Analysis, Leibniz Institute for Age Research, Fritz Lipmann Institute, Jena, Germany; ‡Institute for Molecular and Cellular Anatomy, University of Regensburg, Regensburg, Germany; §Department of Cellular and Molecular Pathology, German Cancer Research Center, Heidelberg, Germany; and ‖Faculty of Biology and Pharmacy, Friedrich Schiller University of Jena, Jena, Germany

ABSTRACT

The *Wilms' tumor suppressor gene 1* (*WT1*) encodes a zinc finger transcription factor. Mutation of *WT1* in humans leads to Wilms' tumor, a pediatric kidney tumor, or other kidney diseases, such as Denys–Drash and Frasier syndromes. We showed previously that inactivation of *WT1* in podocytes of adult mice results in proteinuria, foot process effacement, and glomerulosclerosis. However, the WT1-dependent transcriptional network regulating podocyte development and maintenance *in vivo* remains unknown. Here, we performed chromatin immunoprecipitation followed by high-throughput sequencing with glomeruli from wild-type mice. Additionally, we performed a cDNA microarray screen on an inducible podocyte–specific WT1 knockout mouse model. By integration of cistromic and transcriptomic analyses, we identified the WT1 targetome in mature podocytes. To further analyze the function and targets of *WT1* in podocyte maturation, we used an *Nphs2-Cre* model, in which *WT1* is deleted during podocyte differentiation. These mice display anuria and kidney hemorrhage and die within 24 hours after birth. To address the evolutionary conservation of WT1 targets, we performed functional assays using zebrafish as a model and identified *Nphs2*, *Mafb*, and *Magi2* as novel WT1 target genes required for podocyte development. Our data also show that both *Mafb* and *Magi2* are required for normal development of the embryonic zebrafish kidney. Collectively, our work provides insights into the transcriptional networks controlled by WT1 and identifies novel WT1 target genes that mediate the function of WT1 in podocyte differentiation and maintenance.

J Am Soc Nephrol 26: 2118–2128, 2015. doi: 10.1681/ASN.2014080819

The essential function of the kidney is to filter blood and maintain fluid homeostasis in the body. The podocyte, which surrounds blood capillaries with interdigitating foot processes in Bowman's capsule, is an important component of the filtration apparatus. A specialized intercellular junction called the slit diaphragm is formed between neighboring foot processes to prevent macromolecules from diffusing into the urinary space.[1] Podocytes arise from epithelial precursors during different stages of kidney development, namely the renal vesicle, the S-shaped body, the capillary loop, and the maturing glomeruli stages. Podocytes start to differentiate and establish their intricate architecture, including foot processes and slit diaphragms, from the capillary

Received August 22, 2014. Accepted October 10, 2014.

Published online ahead of print. Publication date available at www.jasn.org.

Correspondence: Prof. Christoph Englert, Molecular Genetics, Leibniz Institute for Age Research, Fritz Lipmann Institute, Beutenbergstrasse 11, 07745 Jena, Germany. Email: cenglert@fli-leibniz.de

stage.[2] Podocytes are terminally differentiated cells with limited capability to proliferate, and podocyte injury or loss is a hallmark of progressive kidney disease.[3] Mutations in genes encoding podocyte differentiation markers, such as Nephrin, Podocin, and PLCε1, give rise to early onset proteinuria and kidney failure.[4–6]

The *Wilms' tumor suppressor 1* (*WT1*) was shown to be mutated in Wilms' tumor, the most common solid pediatric kidney tumor.[7–10] *WT1* mutations are present in approximately 20% of patients with sporadic Wilms' tumor.[11] Mutations in *WT1* have also been shown to occur in several human diseases, such as WAGR, Denys–Drash, and Frasier syndromes which all show glomerular defects, suggesting that the gene has important roles in glomerular development and podocyte function.[12–14] *WT1* is expressed during different stages of the developing kidney. *WT1* expression levels rise significantly as kidney development proceeds, are highest at the capillary stage, and are restricted to podocytes in the adult.[15] *WT1* inactivation in the mouse results in embryonic lethality along with agenesis of kidneys and gonads.[16]

WT1 encodes a transcription factor with an amino-terminal proline- and glutamine-rich protein interaction domain and four carboxy-terminal Krüppel-type (Cys_2-His_2) zinc fingers. *WT1* comprises 10 exons and encodes at least 36 isoforms resulting from alternative splicing, usage of alternative translation start sites, and RNA editing.[17] The most prominent alternative splicing occurs at two splice donor sites of exon 9, resulting in inclusion or exclusion of the three amino acids lysine, threonine, and serine (KTS) between zinc fingers 3 and 4. The corresponding proteins are named WT1+KTS or WT1−KTS, with the latter being considered as a *bona fide* transcription factor.[18] In contrast, WT1+KTS isoforms preferentially bind RNA.[19] To address the requirement of *WT1* at different stages of kidney development and maturation, we generated a conditional *WT1* allele. Podocyte-specific knockout of *WT1* in adult mice results in proteinuria, foot process effacement, and FSGS.[20] However, the molecular role of WT1 in podocyte differentiation and maintenance is largely unknown. Here, we have identified the WT1 direct targetome in podocytes as well as WT1 target genes that are required for podocyte differentiation and homeostasis.

RESULTS

Genomic Characterization of WT1 Targets in Adult Kidney

To identify DNA-binding sites of WT1 across the genome of podocytes, we performed chromatin immunoprecipitation followed by high-throughput sequencing (ChIP-Seq) from isolated mouse glomeruli. We performed two independent ChIP-Seq experiments and obtained a minimum of 10 million reads per sample (Supplemental Table 1). Significantly enriched WT1-occupied peaks were analyzed by the model-based analysis of ChIP-Seq algorithm.[21] Overall, in the two experiments, we identified 4335 and 4956 significantly enriched regions by the cutoff of $P<0.001$. Among those, 2257 peaks were identical in both ChIP-Seq experiments (Figure 1A); 69.3% of WT1 binding sites localized in the promoter and transcribed regions (Figure 1B). WT1 binding sites were significantly enriched in the proximity of transcription start site (TSS) and promoter regions (within 1 kb from TSS [14.3%; $P<0.001$]) (Figure 1, C and D). However, 50% of the mapped WT1 peaks are at least 50 kb away from the closest TSS (Supplemental Figure 1). These results show that WT1 gene regulation works by both proximal and distal regulatory elements. Next, we sought to identify WT1 binding motifs within the central 200 bp of the WT1-binding regions from the overlapping peaks using the MEME-ChIP algorithm (multiple EM for motif elicitation of large DNA datasets) ($P<0.001$).[22] We identified the core consensus sequence *GGGAGG* as the most highly conserved WT1 binding sequence in the two most enriched motifs (called primary and secondary motifs) (Figure 1E). Interestingly, over 85% of peak fragments analyzed contained both primary and secondary motifs, which tended to occur close to one another (Figure 1F).

To identify potential WT1 target genes in podocytes, we selected those genes that showed WT1 binding sites within their transcribed region, including sequences 3 kb upstream of their annotated TSSs. With these criteria, we identified 1573 protein-coding genes and 61 noncoding genes as potential WT1 target genes (Supplemental Table 2). To interpret the biologic significance of WT1 binding sites in adult podocytes, we used the Cytoscape software, identifying the biologic processes and molecular functions enriched in our dataset (Figure 1G).[23] The most highly enriched function related to actin filament organization, indicating that WT1 regulates expression of cytoskeletal components in podocytes. Interestingly, one of highest ranking clusters is glomerular development, which contains *Myo1e*, *Notch2*, *Plce1*, *Ptpro*, etc. Thus, the functions of WT1 targets are consistent with the established role of WT1 in podocytes and thus, serve as an indicator for the quality of our dataset.

WT1 Maintains Podocytes Function as both an Activator and a Repressor

To determine the functional consequence of WT1 activity in mature podocytes, we sought to integrate our WT1 target list with gene expression data. We used quadruple transgenic mice (*$WT1^{fl/fl}$;Nphs2-rtTA;LC1*), which allow us to delete WT1 in adult kidneys on doxycycline induction.[20] To minimize secondary or tertiary effects, we isolated glomeruli with a magnetic bead perfusion method after 6 days of induction of *WT1* deletion. At this time point, the respective knockout mice display slight proteinuria (Supplemental Figure 2). To identify downstream genes of WT1 in podocytes, we performed an exon-array experiment on glomeruli on *WT1* deletion. We observed 1753 differentially expressed genes after knockout of WT1 in adult podocytes by using a P value≤0.05 as a cutoff (Figure 2A, Supplemental Table 3). These genes were analyzed for their molecular and cellular functions and involved KEGG (Kyoto encyclopedia of genes and genomes) pathways using the bioinformatic tool DAVID[24] (Supplemental Table 4). The

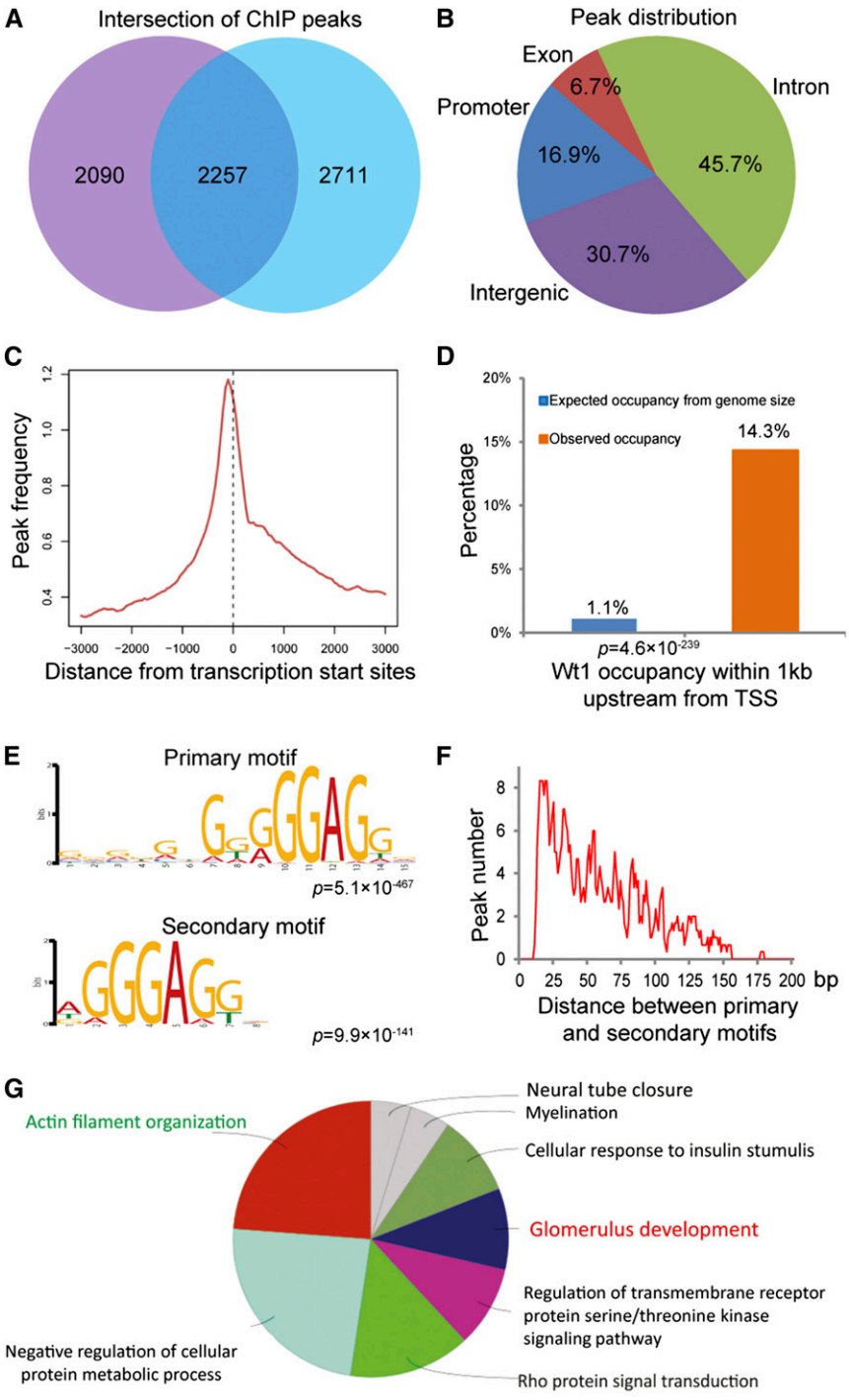

Figure 1. ChIP-Seq reveals WT1 binding to genes regulating podocyte function. (A) The Venn diagram depicts overlapping peaks of the significantly enriched genomic intervals of two biologic replicates of ChIP-Seq from the adult mouse kidney. (B) The genomic distribution of the WT1 ChIP enrichment signal. Classification is on the basis of the following descriptions. Promoter is within 3 kb upstream of TSS, and intergenic is between annotated genes (excluding promoter regions). (C and D) The ChIP enrichment signal is highest near the TSS and highly localized within 1 kb of TSSs. (E) Primary and secondary WT1 binding motifs identified by MEME from the top 500 overlapping peaks. (F) The number of base pairs between primary and secondary motifs. (G) Gene ontology analysis of WT1 cistrome by defining the peaks localized to promoters or gene-transcribed regions. MEME, multiple Em for motif elicitation.

analysis identified axon guidance, lysosome, and focal adhesion as the top three categories among the known affected biologic functions.

Integrating our WT1 ChIP-Seq data with our microarray expression dataset, 192 genes were common to both gene lists. Although most of these genes were downregulated in WT1 knockout glomeruli (148), there were also 44 genes that were upregulated. This indicates that WT1 acts as both an activator and a repressor of transcription (Figure 2B). The WT1 binding motif is identical in both instances, and the position of the WT1 binding region relative to the TSS of genes did not show a difference between activated and repressed genes (data not shown). To identify potential cofactors that could modulate the activating or repressive function of WT1, we masked the identified WT1 binding motifs to search for other consensus motifs that were overrepresented in its proximity. We identified enriched motifs for potential WT1 coactivators, including Sox5, Sox7, and some Fox proteins (*e.g.*, FoxP1 and FoxP2) as potential corepressors (Supplemental Figure 3).[25] The intersection of the WT1 targetome that we identified here with genes reported to be specifically expressed in podocytes[26] revealed that WT1 mostly activates podocyte-enriched genes and represses nonpodocyte-enriched genes (72% activation versus 16% repression) (Supplemental Figure 4). Because our data are derived from adult kidneys, they suggest a role for WT1 in defining and maintaining podocyte identity. Consistent with previous reports, we verified WT1 binding to the promoter of known transcriptional target genes of WT1, such as *Nphs1*[27,28] or *Sulf1*.[29,30] Expression levels of both genes were significantly reduced in WT1 knockout mice (Supplemental Figure 5). Bioinformatic analysis of the common gene list revealed the most affected pathways as regulation of cytoskeleton followed by focal adhesion and tight junction (Figure 2C). Examination of the WT1-deleted mouse podocytes displayed widening and flattening of the foot processes as well as interruption of the slit diagram (Figure 2D).[20] The glomerular basement membrane and its charge seemed unaffected by the podocyte-specific inactivation of *WT1* as shown in electron microscopic

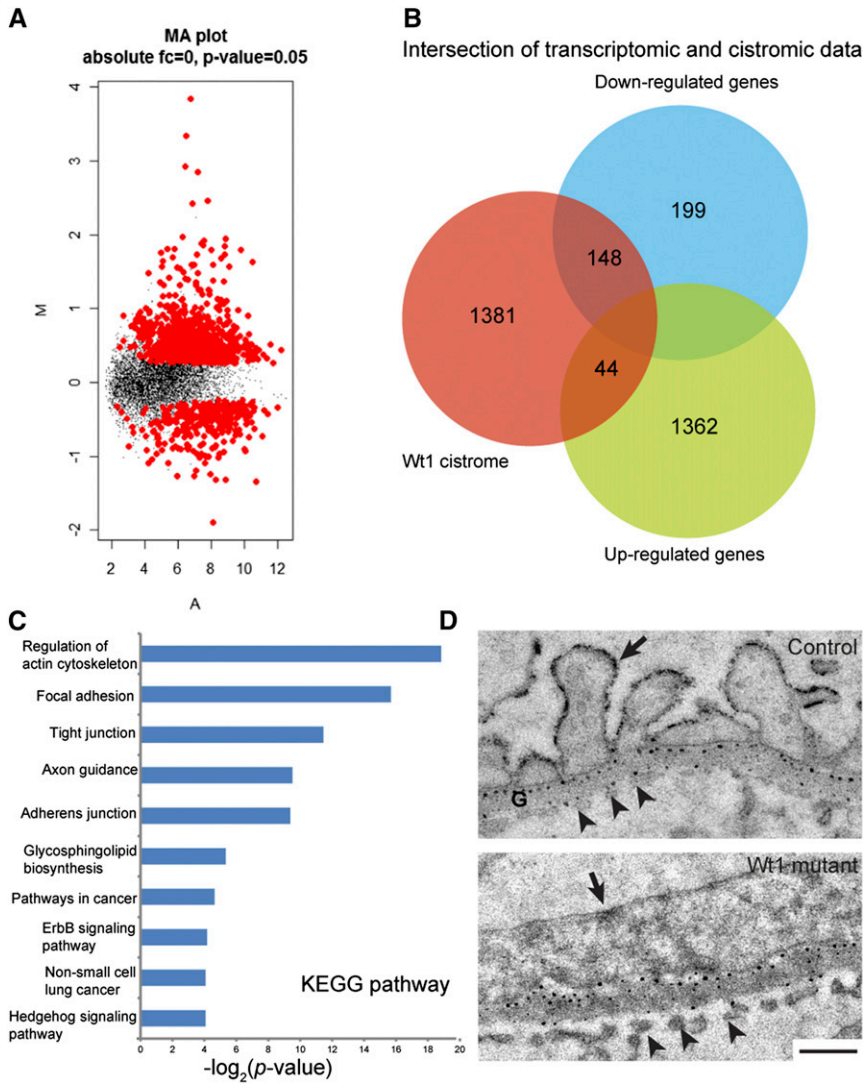

Figure 2. WT1 maintains podocyte function as both an activator and a repressor. (A) The differential expression MA (log_2[fold changes] to average intensity) plots between WT1 mutant and control glomeruli. (B) The Venn diagram depicts the overlapping genes of the WT1 cistrome and up- or downregulated genes in WT1 mutant mice. (C) KEGG pathway enrichment analysis of the WT1 targetome. Overrepresented KEGG pathways are shown in the histogram. (D) Ultrastructural kidney analysis of WT1 mutant and control adult mice (age>8 weeks old) treated with doxycycline for 6 days. Podocytes (arrows) and endothelial cells (arrowheads) were abnormally distant from the glomerular basement membrane (G), which was itself irregularly shaped in the mutant. Black dots indicate negative charges by polyethylenimine staining. No obvious charge differences between the glomerular basement membranes of mutant and control glomeruli are detectable. Scale bar, 0.5 μm. KEGG, Kyoto encyclopedia of genes and genomes; MA, M (log ratios) and A (mean average) scale.

analyses (Figure 2D). These morphologic changes of *WT1* mutant podocytes are, thus, consistent with WT1-controlling genes that are involved in pathways that regulate, for example, the cytoskeleton or cell-cell interaction as mentioned above.

WT1 Is Required for Podocyte Maturation

Human patients with Denys–Drash and Frasier syndromes exhibit glomerular defects caused by mutations in *WT1*.[13,14] This led us to dissect the function of WT1 in maturing podocytes and their maintenance. We and others have shown the requirement of WT1 for podocyte homeostasis.[20,30] However, the role of WT1 in podocyte maturation remains to be illustrated. Here, we used conditional podocyte–specific *WT1* knockout mice (*WT1*$^{fl/fl}$*;Nphs2-Cre*), in which *Cre* expression is driven by a fragment of the *Nphs2* promoter. *Nphs2* is expressed during podocyte maturation after the capillary loop stage.[30] In *WT1*$^{fl/fl}$*;Nphs2-Cre* mice, *WT1* is detected at the capillary loop stage but not in mature glomeruli (Figure 3, A and B). Mutant mice were born at the expected Mendelian ratio but died within 24 hours after birth. Newborn animals suffered from anuria and kidney hemorrhage. Apart from this, the urogenital system displayed no gross abnormalities. On the histologic level, kidneys of *WT1*$^{fl/fl}$*;Nphs2-Cre* mice were characterized by a significant reduction in the number of mature glomeruli and proximal convoluted tubuli (Figure 3, C and D). Given the effect of podocyte-specific *WT1* inactivation on functional kidney architecture, we addressed the question of structural defects regarding podocytes. Indeed, analysis using electron microscopy revealed structural changes in the form of abundant foot process effacement in knockout mice (Figure 3F, arrow). Detachment or loss of podocytes from the vascular tuft, which was detected in histologic analyses, could also be observed in ultrastructural studies (Figure 3H, arrowheads). These data show that WT1 regulates podocyte maturation and that loss of WT1 in podocytes results in failure of the renal filtration system.

WT1 Activates Expression of *Nphs2*, *Mafb*, and *Magi2* in Podocytes

To characterize the genes that mediate the function of WT1 in podocytes, we first sorted the genes by ChIP peaks localized in the promoter (≤1500 bp from TSS) according to foldness of enrichment and only considered peaks with an enrichment of ≥20-fold. Then, using our microarray analysis, only genes that were downregulated on WT1 knockout (and therefore, normally activated by WT1) were used. Of those genes, we selected three for additional analysis; *Nphs2*, *Mafb*, and *Magi2*. WT1 binds to a consensus motif in the promoter region of all of the three genes (Figure 4, A–C). Mutation of *NPHS2* in humans causes nephrotic syndrome.[5]

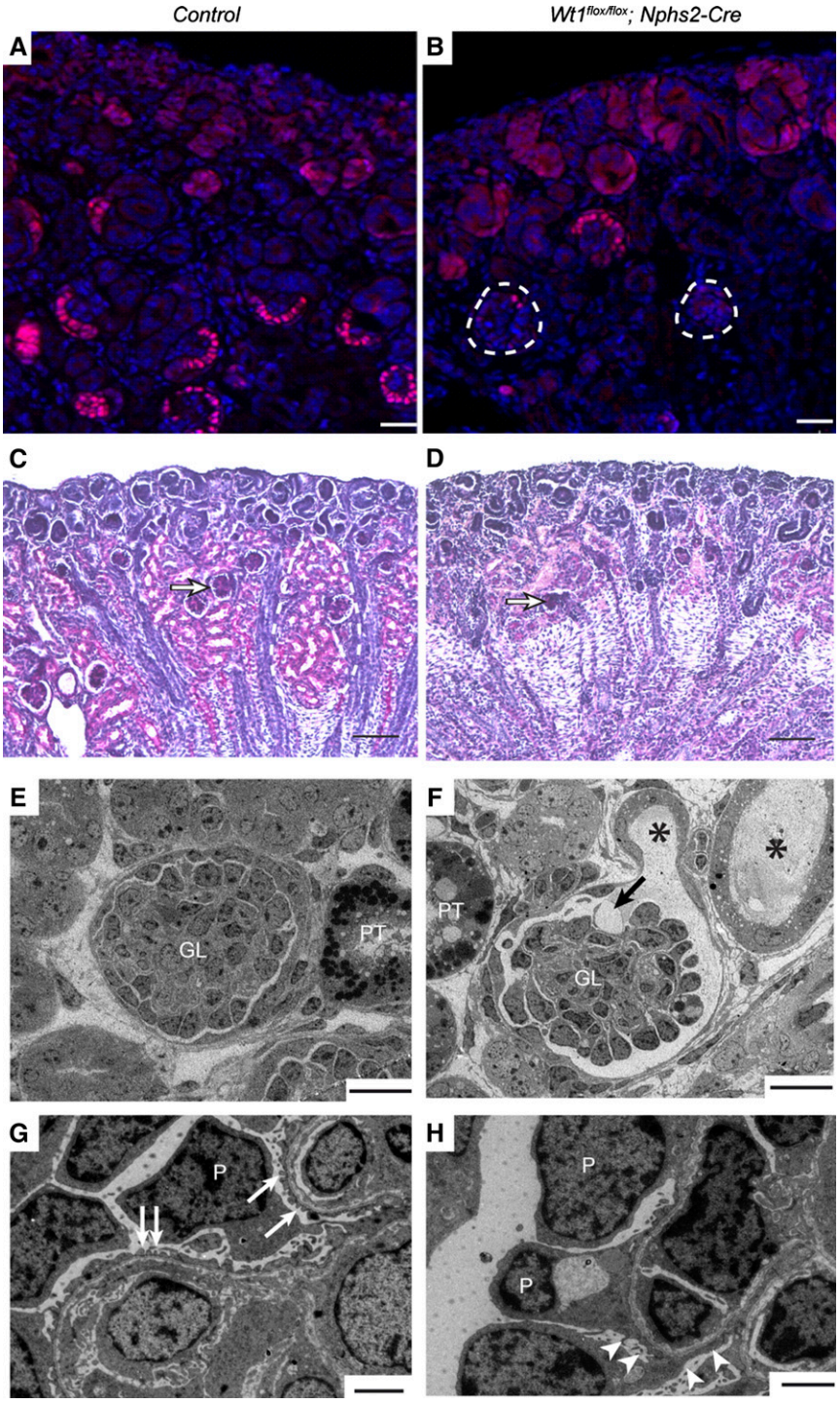

Figure 3. WT1 is required for podocyte differentiation. (A and B) Immunohistochemistry of E18.5 kidney sections using an antibody against WT1 (red) shows disappearance of WT1 signal in glomeruli of mutant mice (dotted lines) and the *WT1*$^{flox/flox}$ mouse as a control. (C and D) Histologic analysis of sagittal kidney sections from newborn (P0) control and *WT1*$^{flox/flox}$*;Nphs2-Cre* mice stained with periodic acid–Schiff (PAS). In kidneys of mutant mice, the numbers of mature glomeruli and proximal convoluted tubuli were strongly reduced. Remaining glomeruli were smaller (arrow). The developmental zone or outer renal cortex was without obvious pathologic findings. (E–H) Ultrastructural kidney analysis from the inner cortex of newborn *WT1*$^{flox/flox}$*;Nphs2-Cre* and control mice. (E) Electron microscopy of a P0 *WT1*$^{flox/+}$*;Nphs2-Cre* control kidney section showing single glomerulus (GL) and convoluted proximal tubulus (PT) of normal appearance. (G) High magnification identifies podocytes (P) with abundant foot processes (arrows). (F) Section of a P0 *WT1*$^{flox/flox}$*;Nphs2-Cre* kidney depicting a glomerulus with one capillary vessel deprived of surrounding podocytes (arrow). Proteinaceous material (asterisks) was found in Bowman's space and neighboring tubuli. (H) High magnification of F reveals widespread foot process effacement (arrowheads). Scale bar, 25 μm in A, B, E, and F; 2 μm in G and H.

Mafb encodes a transcription factor that is expressed at the capillary loop stage and restricted to podocytes as shown in the GUDMAP database.[31] *Mafb* has been shown to be required for podocyte development in mice.[32,33] Magi2 is a component of the slit diaphragm complex and might have a function for the glomerular filtration barrier.[34] Indeed, *Magi2* null mice display morphologic abnormalities of podocytes and anuria.[35] Inactivation of *WT1* resulted in loss of Podocin, Mafb, and Magi2 in podocytes (Figure 4, D–L).

Nphs2, *mafba*, and *magi2* Are Conserved Functional Target Genes of WT1 in Zebrafish

To address the evolutionary conservation of WT1 targets *in vivo*, we turned to zebrafish, which have been frequently used to study podocyte formation during kidney development.[36] Bioinformatic analysis identified single *Nphs2* and *Magi2* genes and two orthologs for *Mafb* in the zebrafish genome. *Nphs2*,[37] *mafba*,[38] and *magi2* were found to be expressed in the glomerular region of the embryonic zebrafish kidney: the pronephros (Figure 5, A–C). *Mafbb* expression was not detectable in this region (Supplemental Figure 6). To determine whether regulation by WT1 was conserved, we examined *nphs2*, *mafba*, and *magi2* activity after *wt1a* and *wt1b* knockdown. Expression levels of *nphs2*, *mafba*, and *magi2* were significantly reduced or absent in both morphants (Figure 5, D–I). This finding encouraged us to study the function of *nphs2*, *mafba*, and *magi2* by knockdown of the respective genes. The injection of

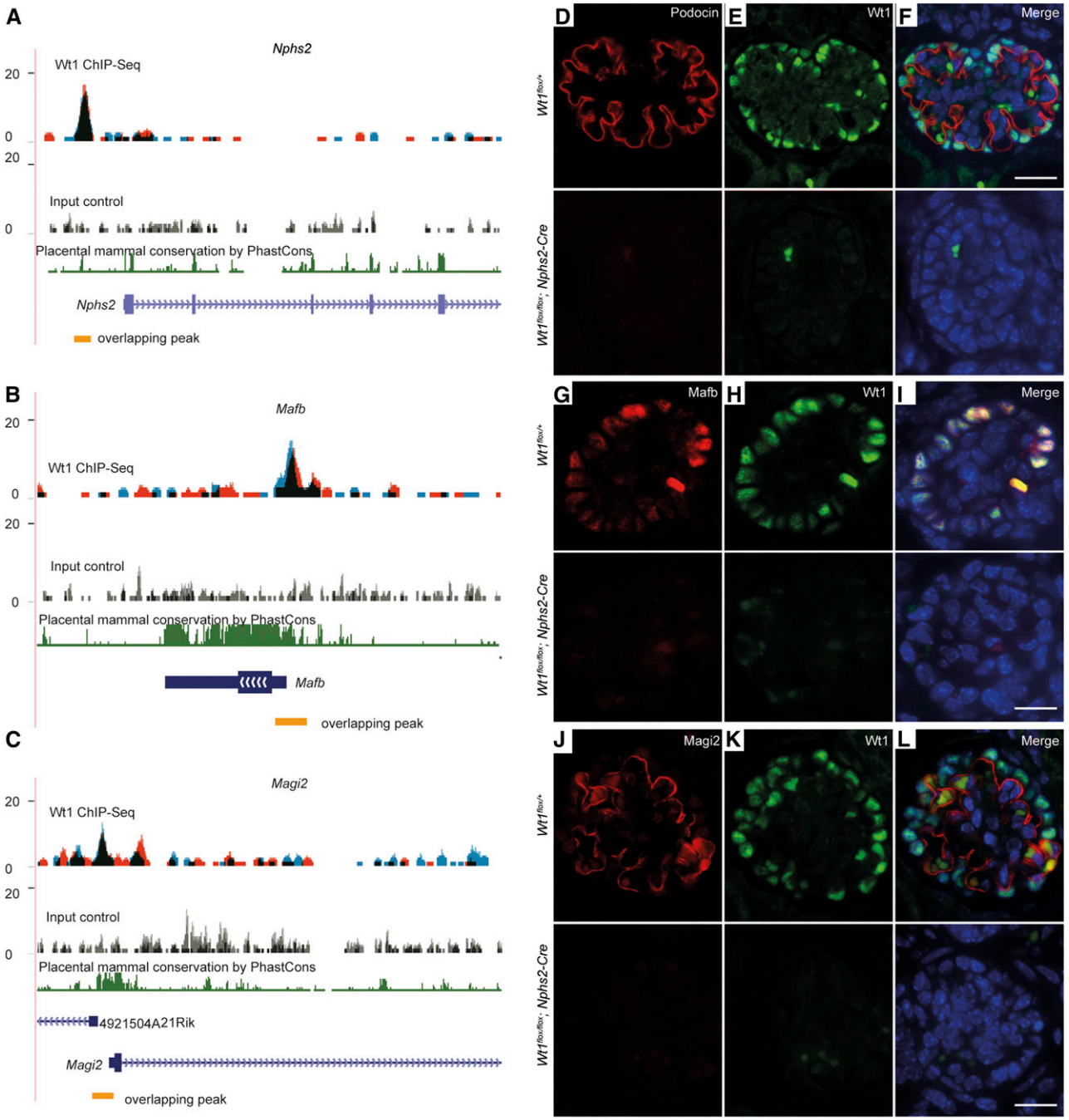

Figure 4. WT1 binds to the promoters and activates expression of *Nphs2*, *Mafb*, and *Magi2* in podocytes. (A–C) Binding of WT1 to the promoters of *Nphs2*, *Mafb*, and *Magi2* as viewed in the University of California-Santa Cruz genome browser within the indicated genomic intervals. ChIP fragment sequences on DNA are shown in red and blue for the two independent WT1 ChIP-Seq datasets. Regions with overlaps are depicted in black. The peaks in the *Nphs2*, *Mafb*, and *Magi2* loci are shown by yellow bars. Input control represents sequencing data of chromatin that were not subjected to immunoprecipitation. Conservation denotes placental mammal basewise conservation by Phastcons score. (D–L) Double immunostaining for WT1 and Podocin, Mafb, and Magi2 in glomeruli of (upper panel) $WT1^{flox/flox}$ or (lower panel) $WT1^{flox/flox}$;*Nphs2-Cre* mice. Scale bar, 10 μm.

antisense morpholinos against *nphs2*,[37] *mafba*, and *magi2* resulted in severe pericardial edema (Figure 5, K–M), which is similar to what is seen in *wt1a/b* morphants.[39] To visualize potential glomerular defects in *nphs2*, *mafba*, and *magi2* knockdown zebrafish embryos, we extended our experiments to the transgenic zebrafish line *wt1b::GFP*, which expresses *GFP* in the developing glomerulus and pronephric tubule.[39] At 48 hours postfertilization, the *nphs2*, *mafba*, and *magi2*

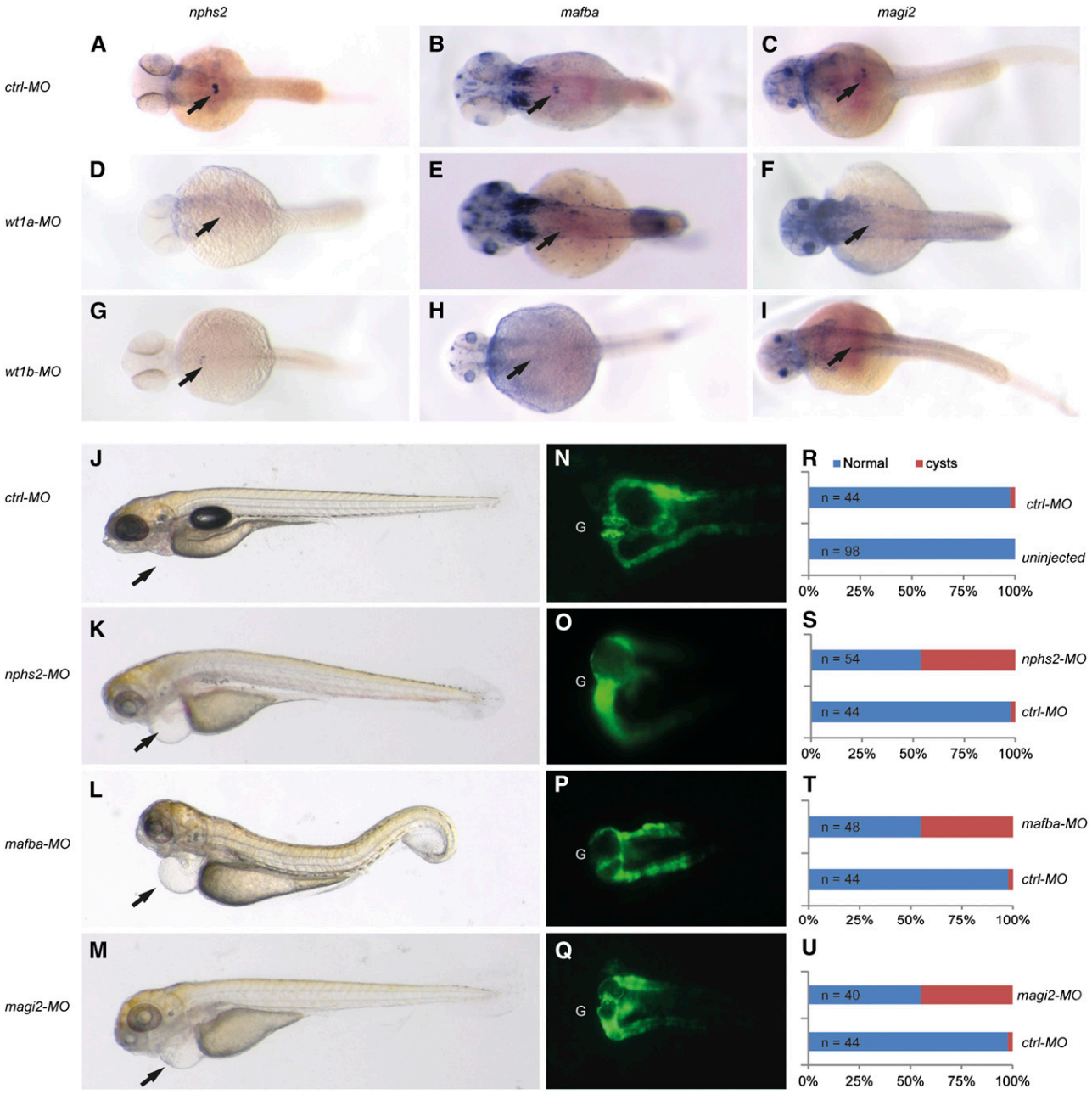

Figure 5. WT1 regulates *nphs2*, *mafba*, and *magi2* expression during pronephros development in zebrafish. (A–C) *nphs2*, *mafba*, and *magi2* are expressed in glomeruli of zebrafish embryos (arrows). (D–I) *nphs2*, *mafba*, and *magi2* expressions are reduced in *wt1a* and *wt1b* morphants (arrows). (J–M) Knockdown of *nphs2*, *mafba*, or *magi2* results in pericardial edema (arrows). (N–U) Knockdown of *nphs2*, *mafba*, or *magi2* in zebrafish results in cyst formation as visualized using a transgenic *wt1b::GFP*.[39] G, glomeruli; GFP, green fluorescent protein; MO, morpholino.

morphants displayed significant pronephros defects, which were visible as glomerular cysts (Figure 5, N–U). The strong effects observed after knockdown of *nphs2*, *mafba*, and *magi2* in developing zebrafish embryos support the notion that, like Podocin, Mafb and Magi2 are regulators of pronephros development in zebrafish. Moreover, loss of expression of all three genes in *wt1a* and *wt1b* morphants shows that Nphs2, Mafb, and Magi2 are conserved target genes of WT1 in podocytes.

DISCUSSION

Several human glomerular diseases are caused by *WT1* mutations, including missense mutation within exon 8 or 9 encoding zinc fingers 2 or 3 in children with Denys–Drash syndrome or alterations of alternative splicing of WT1+KTS and WT1−KTS leading to Frasier syndrome. Both are characterized by nephrotic syndrome associated with glomerulosclerosis.[13,14] The latter is

the end point of a series of processes with podocyte damage or loss as a common denominator.[40] We and others had shown that deletion of *WT1* in adult podocytes results in proteinuria, foot process effacement, and glomerulosclerosis.[20,41] However, the WT1-dependent transcriptional network that governs podocyte differentiation and maintenance remains to be deciphered. In this study, we integrated the WT1 cistrome and transcriptome to provide insight into the complex role of WT1 in podocyte maintenance. In addition, we analyzed the function of WT1 in podocyte differentiation by using a podocyte-specific knockout mouse model. Experiments in zebrafish confirmed the role of selected WT1 target genes in kidney development.

Our ChIP-Seq data analysis revealed WT1 primary and secondary motifs to harbor a core *GGGAGG* sequence that shows high similarity to previously published motifs that had been identified using ChIP on chip or restriction enzyme assistant ChIP-Seq experiments on the developing mouse kidney at E18.5.[42,43] The most striking difference is that we found two similar motifs close to each other in many peak fragments. This suggests that two or more WT1 molecules bind to the same promoter fragment or that WT1 binds as a dimer. In fact, there is evidence that WT1 functions as a homodimer.[44] Dimerization is mediated by two distinct domains within the N-terminal region.[45] Our data also show that, in many cases, binding sites for members of the Sox and Fox families can be found close to WT1 binding sites, showing that WT1 acts in concert with other transcription factors.

Visceral epithelial cells (podocytes) are derived from the cap mesenchyme, wherein *WT1* is expressed at low levels. *WT1* expression increases in pretubular aggregates and is thought to drive cells to undergo the mesenchymal-to-epithelial transition by activating *Wnt4*.[46] *WT1* expression continues to increase along with development of podocyte progenitors and is later restricted to adult podocytes.[15] The integrity of podocytes and their interaction with the glomerular basement membrane are crucial for maintenance of the intact glomerular filtration barrier. Alteration of the intercellular junctions and cytoskeletal structure of podocytes or their detachment from the membrane results in the development of albuminuria.[47] Interestingly, WT1 direct target genes in podocytes were enriched for regulation of actin cytoskeleton, focal adhesion, tight junction, and adherens junction, indicating that WT1 is a central regulator of podocyte architecture. This is corroborated by the podocyte-specific WT1 knockout mouse model that we used, where the loss of WT1 affected podocyte differentiation and led to kidney failure and death within 24 hours after birth.

In this study, we focused on the characterization of the WT1 targets *Nphs2*, *Mafb*, and *Magi2*. Podocin is a key protein of the podocyte slit diaphragm protein complex, where it interacts with nephrin, NEPH1, and CD2AP.[48,49] Mutations in the human podocin gene *NPHS2* cause a corticosteroid-resistant nephrotic syndrome owing to the disruption of filtration barrier integrity.[5] Podocin function is highly conserved between the zebrafish pronephros and the mammalian metanephros.[37] Mafb, a basic leucine zipper transcription factor, is essential for podocyte differentiation and foot process formation, which was suggested by investigation of *Mafb*-deficient mice.[32,33] A recent study revealed that mutations causing alterations in the amino-terminal transcriptional activation domain of MAFB cause multicentric carpotarsal osteolysis (MCTO) characterized by aggressive osteolysis particularly affecting the carpal and tarsal bones. Also, MCTO is frequently associated with progressive renal failure. The pathogenesis of MCTO might be attributed to MAFB dysfunction in osteoclasts and podocytes.[50] *Mafba*, an ortholog in zebrafish, is expressed during early stages of podocyte formation.[38] In this work, we show that *mafba* is required for podocyte development in zebrafish.

Magi2, encoding the membrane-associated guanylate kinase inverted 2, is upregulated on foot process differentiation and consistently expressed in adult podocytes.[34,51] Magi2, together with IQGAP1, CASK, spectrins, and α-actinin, is a component of the nephrin multiprotein complex.[34] A recent study has shown that deletion of the *Magi2* gene in mice causes neonatal lethality with podocyte morphologic abnormalities and anuria.[35] We show here that *magi2* is also expressed in podocytes of zebrafish. Knockdown of *magi2* in zebrafish results in glomerular defects and epicardial edema. In addition, WT1 targets include most genes responsible for hereditary podocyte diseases, such as *NPHS1*, *LAMB2*, *LMX1b*, and even *WT1* itself (Supplemental Table 5).

In summary, our results show that WT1 is a crucial transcription factor for podocyte maturation and maintenance. It fulfills its function by regulation of a number of key target genes, including *Nphs2*, *Mafb*, and *Magi2*. Future work will have to identify the individual contributions of each target gene (*e.g.*, by forcing its expression in WT1-negative podocytes *in vivo*).

CONCISE METHODS

Generation of the Mutant Mice

The inducible podocyte–specific WT1 knockout mouse line (*WT1$^{fl/fl}$;Nphs2-rtTA;LC1*) was generated as described.[20] To inactivate *WT1*, mice were fed with 2 mg/ml doxycycline in a 5% sucrose solution. The conditional podocyte–specific WT1 knockout mouse line (*WT1$^{fl/fl}$;Nphs2-Cre*) was generated by crossing *WT1flox* mice to the transgenic *Nphs2-Cre* mice.[52] All animal experiments were performed in accordance with institutional guidelines and ethical review committees.

ChIP-Seq

Briefly, glomeruli were isolated from 2- to 3-month-old C57BL/6 mice using the sieving method.[53] Glomeruli were fixed with 1% formaldehyde for 15 minutes at 37°C, washed with 125 mM glycine, resuspended in ChIP buffer (150 mM NaCl, 50 mM Tris-HCl, pH 7.5, 5 mM EDTA, 0.5% NP-40, 0.1% SDS, and 1.0% Triton X-100) containing protease inhibitors (Roche), and sonicated with the Bioruptor for 30 minutes (30 seconds on and 30 seconds off). WT1 immunoprecipitation was performed as described[54] using the C-19 antibody

(Santa Cruz Biotechnology). DNA was eluted with the Qiagen MinElute PCR Purification Kit. Templates for ChIP-Seq analysis were prepared using the TruSeq ChIP Sample Prep Kit (Illumia) following the manufacturer's instructions. Sequencing was performed on an Illumina HiSeq2000 platform, and at least 10 million reads of 50-nucleotide single-end sequences were generated for each sample. The sequences were mapped to the mouse genome (version mm10), allowing two base mismatches. Peak calling was carried out using model-based analysis of ChIP-Seq.[55] Peaks were considered identical when they showed an overlap of at least 6 bp. WT1 binding motif was carried out using MEME.[22]

Microarray

Two sets of six 2- to 3-month-old mice with each of the following genotypes (*WT1$^{flox/flox}$;Nphs2-rtTA;LC-1* and *WT1$^{flox/flox}$;Nphs2-rtTA*) were treated for 6 days with doxycycline in the drinking water. Subsequently, glomeruli were extracted using magnetic bead perfusion.[56] RNA was isolated from the glomeruli using the RNeasy Mini Kit (Qiagen). The resulting RNA was then used to create the biotin-labeled library to be hybridized on GeneChips Exon 1.0 ST mouse microarrays following the procedure described by the manufacturer (Affymetrix). The hybridization data were analyzed using oneChannelGUI.[57] The list of differentially expressed genes was generated using an FDR≤0.05.

Transmission Electron Microscopy

Newborn (P0) mice were euthanized by decapitation, and kidneys were harvested, washed in 1× PBS, fixed in a freshly prepared solution of 2% glutaraldehyde (Sigma-Aldrich) in 1× PBS for 2 d at 4°C, and conserved for 2–4 d in 1× PBS-buffered 0.02% sodium azide (Merck GmbH) at 4°C. Adult mice were deeply anesthetized with xylazine/ketamine and perfused with 40 ml freshly prepared 2% glutaraldehyde/1× PBS through the heart's left ventricle. After isolation, kidneys were cut into small pieces of approximately 1 mm^3 and postfixed in 2% glutaraldehyde/1× PBS for 3–4 d at 4°C. The specimens were incubated with cacodylate-buffered 1% OsO_4 for 2–3 hours before being embedded in Epon. Ultrathin sections were stained with uranyl acetate and lead citrate and then visualized in a transmission electron microscope (Carl Zeiss EM 902) equipped with a cooled CCD digital camera (TRS Tröndle Restlichtverstärkersysteme).

Polyethylenimine Staining

Kidneys of euthanized adult mice were isolated, cut into 1-mm^3 pieces, stained with 0.5% polyethylenimine in 0.9% NaCl (pH 7.3) for 30 minutes, washed with three changes of 50 mM sodium cacodylate for 10 minutes each, fixed in 2% phosphotungstic acid/0.1% glutaraldehyde for 1 hour, washed with 50 mM sodium cacodylate buffer, treated for 2 hours with 1% OsO_4 in 25 mM sodium cacodylate for contrasting, dehydrated, and embedded in EPON 812.

Immunohistochemistry

E18.5 kidneys of *WT1* mutant and control mice were fixed in 4% PFA, embedded in paraffin, and cut into 8-μm sections. The sections were deparaffinized, subjected to antigen retrieval treatment, and blocked for 1 hour at room temperature in 5% normal donkey serum, 1% BSA, and 0.1% Triton X-100 in PBS before the primary antibodies were applied. The following antibodies were used: a polyclonal rabbit antipodocin antibody (diluted 1:100; Sigma-Aldrich), a monoclonal mouse anti-human WT1 antibody (diluted 1:100; Dako), a polyclonal rabbit anti-Magi2 antibody (diluted 1:50; EMD Millipore), and the polyclonal rabbit anti-Mafb antibody (diluted 1:50; Bethyl). After three washes, the sections were stained with an Alexa Fluor 594 goat anti-rabbit IgG antibody (diluted 1:500) or an Alexa 488-conjugated goat anti-mouse IgG antibody (diluted 1:500; Invitrogen) for 1 hour at room temperature. The DNA was visualized using Hoechst staining before mounting slides with ProLong Gold Antifade Mountant (Life Technology). Sections were analyzed with a Carl Zeiss Axio Imager ApoTome. Pictures were taken with a Carl Zeiss AxioCam MRm digital camera.

Zebrafish Maintenance

Zebrafish were maintained under standard conditions for zebrafish husbandry.[58] Embryos were raised at 28°C and staged according to morphologic criteria.[59]

Whole-Mount *In Situ* Hybridization

The cDNA fragment, which was used for the riboprobe of zebrafish *mafba*, was amplified with primer pair 5′-CCACGAGCGACAACCCGTCCT-3′ (forward) and 5′-GTTCCCCCTGTCGCCTCTCTC-3′ (reverse), giving rise to a 510-bp PCR product. The zebrafish *magi2* cDNA fragment was amplified with primers 5′-CCCCCGAAGAATGCAAGGAA-3′ (forward) and 5′-AAGAACAAACTGTGCCTCCTCT-3′ (reverse), giving rise to a 1014-bp PCR product. The *nphs2* probe was used as previously described.[39] Whole-mount *in situ* hybridization was performed as described.[39] Embryos were hybridized with a digoxigenin-labeled riboprobe of *nphs2*, *mafba*, or *magi2*. Anti-DIG AP and NBT/BCIP (Roche) were used to detect the probe. After color reaction, embryos were washed with methanol, equilibrated in clearing solution (1/3 benzoyl-alcohol and 2/3 benzoyl-benzoate), and photographed using a stereomicroscope (SteREO Discovery V8; Zeiss).

Zebrafish Experiments

Antisense morpholino-oligonucleotides (GeneTools) were directed against the translational start site (*mafba* and *magi2*) or the splice donor site of exon 3 (*nphs2*). As a control, a standard morpholino that is directing against a human *β-globin* intron mutation was used. Morpholinos were diluted in water to a working concentration of 1 mM with 0.1% phenol red as a tracer. Dose-response experiments were carried out by injections of 0.1–0.5 nl into the yolk of one- or two-cell embryos using a manual manipulator (type M1; Saur). The following morpholino oligonucleotides were used in this study: *nphs2*, TGCGATTTAAAACGTGTACCAGGGC; *mafba*, CGCTCATCGTGCCCCTGTTCTTCAG; *magi2*, TTTTCTTCTTCAGGCTTTTGGACAT; and *wt1a* and *wt1b* as described[39]; 24, 48, and 72 hours postfertilization, injected embryos were treated with 0.016% tricaine (Sigma) before being evaluated for morphologic defects using the epifluorescence microscope Zeiss SteREO Discovery V8. To determine the lowest morpholino concentration required to induce morphologic defects, injections with increasing morpholino dosage were performed. Images were generated using the AxioVision software (Carl Zeiss).

ACKNOWLEDGMENTS

We thank Abinaya Nathan and Thomas Bates for critically reading and improving this manuscript and Gundula Bergner for secretarial assistance. We also thank Cornelia Luge for chromatin immunoprecipitation followed by high-throughput sequencing library preparation, Jenny Buchelt and Frank Kaufmann for maintenance of the mouse colonies, and Sabrina Stötzer and Christina Ebert for zebrafish husbandry. We thank Maik Baldauf and Gabriele Günther for technical support and many other members of our laboratory for their helpful discussions and contributions.

This work was supported by Deutsche Forschungsgemeinschaft Grants SFB 699 (to R.W.) and EN280/8-1 (to C.E.).

DISCLOSURES

None.

REFERENCES

1. Pavenstädt H, Kriz W, Kretzler M: Cell biology of the glomerular podocyte. *Physiol Rev* 83: 253–307, 2003
2. Dressler GR: The cellular basis of kidney development. *Annu Rev Cell Dev Biol* 22: 509–529, 2006
3. Greka A, Mundel P: Cell biology and pathology of podocytes. *Annu Rev Physiol* 74: 299–323, 2012
4. Kestilä M, Lenkkeri U, Männikkö M, Lamerdin J, McCready P, Putaala H, Ruotsalainen V, Morita T, Nissinen M, Herva R, Kashtan CE, Peltonen L, Holmberg C, Olsen A, Tryggvason K: Positionally cloned gene for a novel glomerular protein—nephrin—is mutated in congenital nephrotic syndrome. *Mol Cell* 1: 575–582, 1998
5. Boute N, Gribouval O, Roselli S, Benessy F, Lee H, Fuchshuber A, Dahan K, Gubler MC, Niaudet P, Antignac C: NPHS2, encoding the glomerular protein podocin, is mutated in autosomal recessive steroid-resistant nephrotic syndrome. *Nat Genet* 24: 349–354, 2000
6. Hinkes B, Wiggins RC, Gbadegesin R, Vlangos CN, Seelow D, Nürnberg G, Garg P, Verma R, Chaib H, Hoskins BE, Ashraf S, Becker C, Hennies HC, Goyal M, Wharram BL, Schachter AD, Mudumana S, Drummond I, Kerjaschki D, Waldherr R, Dietrich A, Ozaltin F, Bakkaloglu A, Cleper R, Basel-Vanagaite L, Pohl M, Griebel M, Tsygin AN, Soylu A, Müller D, Sorli CS, Bunney TD, Katan M, Liu J, Attanasio M, O'toole JF, Hasselbacher K, Mucha B, Otto EA, Airik R, Kispert A, Kelley GG, Smrcka AV, Gudermann T, Holzman LB, Nürnberg P, Hildebrandt F: Positional cloning uncovers mutations in PLCE1 responsible for a nephrotic syndrome variant that may be reversible. *Nat Genet* 38: 1397–1405, 2006
7. Call KM, Glaser T, Ito CY, Buckler AJ, Pelletier J, Haber DA, Rose EA, Kral A, Yeger H, Lewis WH, Jones C, Housman DE: Isolation and characterization of a zinc finger polypeptide gene at the human chromosome 11 Wilms' tumor locus. *Cell* 60: 509–520, 1990
8. Gessler M, Poustka A, Cavenee W, Neve RL, Orkin SH, Bruns GA: Homozygous deletion in Wilms tumours of a zinc-finger gene identified by chromosome jumping. *Nature* 343: 774–778, 1990
9. Haber DA, Buckler AJ, Glaser T, Call KM, Pelletier J, Sohn RL, Douglass EC, Housman DE: An internal deletion within an 11p13 zinc finger gene contributes to the development of Wilms' tumor. *Cell* 61: 1257–1269, 1990
10. Rose EA, Glaser T, Jones C, Smith CL, Lewis WH, Call KM, Minden M, Champagne E, Bonetta L, Yeger H, Housman DE: Complete physical map of the WAGR region of 11p13 localizes a candidate Wilms' tumor gene. *Cell* 60: 495–508, 1990
11. Huff V: Wilms tumor genetics. *Am J Med Genet* 79: 260–267, 1998
12. Narahara K, Kikkawa K, Kimira S, Kimoto H, Ogata M, Kasai R, Hamawaki M, Matsuoka K: Regional mapping of catalase and Wilms tumor—aniridia, genitourinary abnormalities, and mental retardation triad loci to the chromosome segment 11p1305——p1306. *Hum Genet* 66: 181–185, 1984
13. Pelletier J, Bruening W, Kashtan CE, Mauer SM, Manivel JC, Striegel JE, Houghton DC, Junien C, Habib R, Fouser L, Fine RN, Silverman BL, Harber DA, Housman D: Germline mutations in the Wilms' tumor suppressor gene are associated with abnormal urogenital development in Denys-Drash syndrome. *Cell* 67: 437–447, 1991
14. Barbaux S, Niaudet P, Gubler MC, Grünfeld JP, Jaubert F, Kuttenn F, Fékété CN, Souleyreau-Therville N, Thibaud E, Fellous M, McElreavey K: Donor splice-site mutations in WT1 are responsible for Frasier syndrome. *Nat Genet* 17: 467–470, 1997
15. Mundlos S, Pelletier J, Darveau A, Bachmann M, Winterpacht A, Zabel B: Nuclear localization of the protein encoded by the Wilms' tumor gene WT1 in embryonic and adult tissues. *Development* 119: 1329–1341, 1993
16. Kreidberg JA, Sariola H, Loring JM, Maeda M, Pelletier J, Housman D, Jaenisch R: WT-1 is required for early kidney development. *Cell* 74: 679–691, 1993
17. Ozdemir DD, Hohenstein P: WT1 in the kidney—a tale in mouse models. *Pediatr Nephrol* 29: 687–693, 2014
18. Bickmore WA, Oghene K, Little MH, Seawright A, van Heyningen V, Hastie ND: Modulation of DNA binding specificity by alternative splicing of the Wilms tumor wt1 gene transcript. *Science* 257: 235–237, 1992
19. Caricasole A, Duarte A, Larsson SH, Hastie ND, Little M, Holmes G, Todorov I, Ward A: RNA binding by the Wilms tumor suppressor zinc finger proteins. *Proc Natl Acad Sci U S A* 93: 7562–7566, 1996
20. Gebeshuber CA, Kornauth C, Dong L, Sierig R, Seibler J, Reiss M, Tauber S, Bilban M, Wang S, Kain R, Böhmig GA, Moeller MJ, Gröne HJ, Englert C, Martinez J, Kerjaschki D: Focal segmental glomerulosclerosis is induced by microRNA-193a and its downregulation of WT1. *Nat Med* 19: 481–487, 2013
21. Zhang Y, Liu T, Meyer CA, Eeckhoute J, Johnson DS, Bernstein BE, Nusbaum C, Myers RM, Brown M, Li W, Liu XS: Model-based analysis of ChIP-Seq (MACS). *Genome Biol* 9: R137, 2008
22. Machanick P, Bailey TL: MEME-ChIP: Motif analysis of large DNA datasets. *Bioinformatics* 27: 1696–1697, 2011
23. Saito R, Smoot ME, Ono K, Ruscheinski J, Wang PL, Lotia S, Pico AR, Bader GD, Ideker T: A travel guide to Cytoscape plugins. *Nat Methods* 9: 1069–1076, 2012
24. Huang W, Sherman BT, Lempicki RA: Systematic and integrative analysis of large gene lists using DAVID bioinformatics resources. *Nat Protoc* 4: 44–57, 2009
25. Gupta S, Stamatoyannopoulos JA, Bailey TL, Noble WS: Quantifying similarity between motifs. *Genome Biol* 8: R24, 2007
26. Boerries M, Grahammer F, Eiselein S, Buck M, Meyer C, Goedel M, Bechtel W, Zschiedrich S, Pfeifer D, Laloë D, Arrondel C, Gonçalves S, Krüger M, Harvey SJ, Busch H, Dengjel J, Huber TB: Molecular fingerprinting of the podocyte reveals novel gene and protein regulatory networks. *Kidney Int* 83: 1052–1064, 2013
27. Wagner N, Wagner KD, Xing Y, Scholz H, Schedl A: The major podocyte protein nephrin is transcriptionally activated by the Wilms' tumor suppressor WT1. *J Am Soc Nephrol* 15: 3044–3051, 2004
28. Guo G, Morrison DJ, Licht JD, Quaggin SE: WT1 activates a glomerular-specific enhancer identified from the human nephrin gene. *J Am Soc Nephrol* 15: 2851–2856, 2004
29. Schumacher VA, Schlötzer-Schrehardt U, Karumanchi SA, Shi X, Zaia J, Jeruschke S, Zhang D, Pavenstädt H, Drenckhan A, Amann K, Ng C, Hartwig S, Ng KH, Ho J, Kreidberg JA, Taglienti M, Royer-Pokora B, Ai X: WT1-dependent sulfatase expression maintains the normal glomerular filtration barrier. *J Am Soc Nephrol* 22: 1286–1296, 2011

30. Ratelade J, Arrondel C, Hamard G, Garbay S, Harvey S, Biebuyck N, Schulz H, Hastie N, Pontoglio M, Gubler MC, Antignac C, Heidet L: A murine model of Denys-Drash syndrome reveals novel transcriptional targets of WT1 in podocytes. *Hum Mol Genet* 19: 1–15, 2010
31. Davies JA, Little MH, Aronow B, Armstrong J, Brennan J, Lloyd-MacGilp S, Armit C, Harding S, Piu X, Roochun Y, Haggarty B, Houghton D, Davidson D, Baldock R: Access and use of the GUDMAP database of genitourinary development. *Methods Mol Biol* 886: 185–201, 2012
32. Sadl V, Jin F, Yu J, Cui S, Holmyard D, Quaggin S, Barsh G, Cordes S: The mouse Kreisler (Krml1/MafB) segmentation gene is required for differentiation of glomerular visceral epithelial cells. *Dev Biol* 249: 16–29, 2002
33. Moriguchi T, Hamada M, Morito N, Terunuma T, Hasegawa K, Zhang C, Yokomizo T, Esaki R, Kuroda E, Yoh K, Kudo T, Nagata M, Greaves DR, Engel JD, Yamamoto M, Takahashi S: MafB is essential for renal development and F4/80 expression in macrophages. *Mol Cell Biol* 26: 5715–5727, 2006
34. Lehtonen S, Ryan JJ, Kudlicka K, Iino N, Zhou H, Farquhar MG: Cell junction-associated proteins IQGAP1, MAGI-2, CASK, spectrins, and alpha-actinin are components of the nephrin multiprotein complex. *Proc Natl Acad Sci U S A* 102: 9814–9819, 2005
35. Ihara K, Asanuma K, Fukuda T, Ohwada S, Yoshida M, Nishimori K: MAGI-2 is critical for the formation and maintenance of the glomerular filtration barrier in mouse kidney. *Am J Pathol* 184: 2699–2708, 2014
36. Kroeger PT Jr., Wingert RA: Using zebrafish to study podocyte genesis during kidney development and regeneration. *Genesis* 52: 771–792, 2014
37. Kramer-Zucker AG, Wiessner S, Jensen AM, Drummond IA: Organization of the pronephric filtration apparatus in zebrafish requires Nephrin, Podocin and the FERM domain protein Mosaic eyes. *Dev Biol* 285: 316–329, 2005
38. O'Brien LL, Grimaldi M, Kostun Z, Wingert RA, Selleck R, Davidson AJ: WT1a, Foxc1a, and the Notch mediator Rbpj physically interact and regulate the formation of podocytes in zebrafish. *Dev Biol* 358: 318–330, 2011
39. Perner B, Englert C, Bollig F: The Wilms tumor genes wt1a and wt1b control different steps during formation of the zebrafish pronephros. *Dev Biol* 309: 87–96, 2007
40. Mondini A, Messa P, Rastaldi MP: The sclerosing glomerulus in mice and man: Novel insights. *Curr Opin Nephrol Hypertens* 23: 239–244, 2014
41. Chau YY, Brownstein D, Mjoseng H, Lee WC, Buza-Vidas N, Nerlov C, Jacobsen SE, Perry P, Berry R, Thornburn A, Sexton D, Morton N, Hohenstein P, Freyer E, Samuel K, van't Hof R, Hastie N: Acute multiple organ failure in adult mice deleted for the developmental regulator WT1. *PLoS Genet* 7: e1002404, 2011
42. Motamedi FJ, Badro DA, Clarkson M, Lecca MR, Bradford ST, Buske FA, Saar K, Hübner N, Brändli AW, Schedl A: WT1 controls antagonistic FGF and BMP-pSMAD pathways in early renal progenitors. *Nat Commun* 5: 4444, 2014
43. Hartwig S, Ho J, Pandey P, Macisaac K, Taglienti M, Xiang M, Alterovitz G, Ramoni M, Fraenkel E, Kreidberg JA: Genomic characterization of Wilms' tumor suppressor 1 targets in nephron progenitor cells during kidney development. *Development* 137: 1189–1203, 2010
44. Moffett P, Bruening W, Nakagama H, Bardeesy N, Housman D, Housman DE, Pelletier J: Antagonism of WT1 activity by protein self-association. *Proc Natl Acad Sci U S A* 92: 11105–11109, 1995
45. Holmes G, Boterashvili S, English M, Wainwright B, Licht J, Little M: Two N-terminal self-association domains are required for the dominant negative transcriptional activity of WT1 Denys-Drash mutant proteins. *Biochem Biophys Res Commun* 233: 723–728, 1997
46. Essafi A, Webb A, Berry RL, Slight J, Burn SF, Spraggon L, Velecela V, Martinez-Estrada OM, Wiltshire JH, Roberts SG, Brownstein D, Davies JA, Hastie ND, Hohenstein P: A wt1-controlled chromatin switching mechanism underpins tissue-specific wnt4 activation and repression. *Dev Cell* 21: 559–574, 2011
47. Brinkkoetter PT, Ising C, Benzing T: The role of the podocyte in albumin filtration. *Nat Rev Nephrol* 9: 328–336, 2013
48. Schwarz K, Simons M, Reiser J, Saleem MA, Faul C, Kriz W, Shaw AS, Holzman LB, Mundel P: Podocin, a raft-associated component of the glomerular slit diaphragm, interacts with CD2AP and nephrin. *J Clin Invest* 108: 1621–1629, 2001
49. Sellin L, Huber TB, Gerke P, Quack I, Pavenstadt H, Walz G: NEPH1 defines a novel family of podocin interacting proteins. *FASEB J* 17: 115–117, 2003
50. Zankl A, Duncan EL, Leo PJ, Clark GR, Glazov EA, Addor MC, Herlin T, Kim CA, Leheup BP, McGill J, McTaggart S, Mittas S, Mitchell AL, Mortier GR, Robertson SP, Schroeder M, Terhal P, Brown MA: Multicentric carpotarsal osteolysis is caused by mutations clustering in the amino-terminal transcriptional activation domain of MAFB. *Am J Hum Genet* 90: 494–501, 2012
51. Ihara KI, Nishimura T, Fukuda T, Ookura T, Nishimori K: Generation of Venus reporter knock-in mice revealed MAGI-2 expression patterns in adult mice. *Gene Expr Patterns* 12: 95–101, 2012
52. Moeller MJ, Sanden SK, Soofi A, Wiggins RC, Holzman LB: Podocyte-specific expression of cre recombinase in transgenic mice. *Genesis* 35: 39–42, 2003
53. Akis N, Madaio MP: Isolation, culture, and characterization of endothelial cells from mouse glomeruli. *Kidney Int* 65: 2223–2227, 2004
54. Heliot C, Cereghini S: Analysis of in vivo transcription factor recruitment by chromatin immunoprecipitation of mouse embryonic kidney. *Methods Mol Biol* 886: 275–291, 2012
55. Feng J, Liu T, Qin B, Zhang Y, Liu XS: Identifying ChIP-seq enrichment using MACS. *Nat Protoc* 7: 1728–1740, 2012
56. Takemoto M, Asker N, Gerhardt H, Lundkvist A, Johansson BR, Saito Y, Betsholtz C: A new method for large scale isolation of kidney glomeruli from mice. *Am J Pathol* 161: 799–805, 2002
57. Sanges R, Cordero F, Calogero RA: oneChannelGUI: A graphical interface to Bioconductor tools, designed for life scientists who are not familiar with R language. *Bioinformatics* 23: 3406–3408, 2007
58. Westerfield M: The Zebrafish Book. A Guide for the Laboratory Use of Zebrafish (Danio rerio), 3rd Edition *Eugene, OR, University of Oregon Press,385 (Book)* 1995.
59. Kimmel CB, Ballard WW, Kimmel SR, Ullmann B, Schilling TF: Stages of embryonic development of the zebrafish. *Dev Dyn* 203: 253–310, 1995

This article contains supplemental material online at http://jasn.asnjournals.org/lookup/suppl/doi:10.1681/ASN.2014080819/-/DCSupplemental.